# Photoemission studies of oxide superconductors

Egdell, R.G.; Flavell, W.R.; Golden, M.S.

DOI
10.1088/0953-2048/3/1/003
Publication date
1990

Published in
Superconductor Science & Technology

Supercond. Sci. Technol. 3 (1990) 8–19. Printed in the UK

# Photoemission studies of oxide superconductors

**R G Egdell, W R Flavell and M S Golden**
Centre for High Temperature Superconductivity, Department of Chemistry, South Kensington, Imperial College, London SW7 2AZ, UK

Received 21 September 1989

**Abstract.** A procedure has been developed for preparation of clean surfaces of oxide superconductors for study by electron spectroscopy. This involves annealing ceramic or thin film samples under an oxygen atmosphere in a preparation chamber that is an integral part of the spectrometer UHV system. The technique has allowed us to obtain high quality spectroscopic data from $YBa_2Cu_3O_{7-x}$, $Bi_2Sr_2Ca_{n-1}Cu_nO_{4+2n}$ ($n = 2, 3$) and $La_{2-x}Sr_xCuO_4$. Our results are considered in relation to other contemporary work. Current areas of controversy will be highlighted, including a discussion of Fermi edge and satellite structure in valence region spectra and evidence for mixed valency in Cu : 2p and O : 1s core regions.

## 1. Introduction

Following the discovery of superconductivity at temperatures above 30 K in the Ba–La–Cu–O oxide system [1] and the subsequent emergence of 'high temperature' superconductivity in systems including $La_{2-x}Sr_xCuO_4$ [2], $YBa_2Cu_3O_{7-x}$ (for a review of structural work see [3]), $Bi_2Sr_2Ca_{n-1}Cu_nO_{4+2n}$ [4] and $Tl_2Ba_2Ca_{n-1}Cu_nO_{4+2n}$ [5], there have been at least 200 studies of oxide superconductors using electron spectroscopic techniques such as photoemission, Auger electron spectroscopy and energy loss spectroscopy. Motivation to do this work comes in part from the ability of electron spectroscopy, particularly photoemission, to provide detailed information about electronic states, band structure and correlation effects in the new materials.

By virtue of the short inelastic pathlength ($5\ \text{Å} < \lambda < 30\ \text{Å}$) of low energy electrons in solids, electron spectroscopic techniques intrinsically probe only the outermost atomic layers of solid samples. A parallel theme in electron spectroscopic work has therefore been the study of surface phenomena such as reactions of the new materials with atmospheric gases and segregation of dopants and impurities to surfaces and grain boundaries. The effective probing depth in electron spectroscopy nicely matches the short coherence lengths of the new materials [6], so that electron spectroscopic studies are of immediate interest in relation to the behaviour of surfaces and grain boundary interfaces in limiting critical currents. At the same time the surface sensitivity raises problems when attempting to derive information about bulk electronic states and careful attention must be paid to surface cleaning before meaningful spectroscopic measurements can be undertaken. Most surface preparation procedures involve creating a new surface in UHV, using techniques such as cleavage, abrasion or ion milling. In the present paper we describe an alternative method for preparation of clean surfaces of oxide superconductors that allows study of equilibrated external surfaces. We then describe application of this technique to the study of core and valence photoemission of $La_{2-x}Sr_xCuO_4$, $YBa_2Cu_3O_{7-x}$ and $Bi_2Sr_2Ca_{n-1}Cu_nO_{4+2n}$ based materials. Our own results are considered in relation to those reported elsewhere in the literature. Areas of controversy will be identified and a brief survey will be given of the positive contributions that photoemission measurements have made to our understanding of cuprate superconductors.

## 2. Sample pretreatment in electron spectroscopy

Like many other oxides, the new superconductors are susceptible to reaction with atmospheric $CO_2$ and $H_2O$ to give surface carbonate and hydroxide species. The behaviour of $YBa_2Cu_3O_{7-x}$ has been studied in particular detail using a range of techniques including x-ray diffraction [7], Raman scattering, infrared reflectance and x-ray photoelectron spectroscopy (XPS) [8]. It transpires that the dominant surface reaction is

$$2YBa_2Cu_3O_7 + 3CO_2 \rightarrow Y_2BaCuO_5 + 3BaCO_3 + 5CuO + \tfrac{1}{2}O_2.$$

This is strongly catalysed by water vapour.

Degradation reactions of other superconductors are less well studied, although in the case of $La_{2-x}Sr_xCuO_4$, $La(OH)_3$ has been identified in Raman spectra after exposure of samples to moist air [9], whilst XPS studies of $Bi_2(Sr, Ca)_3Cu_2O_8$ point to the presence

0953-2048/90/010008 + 12 $03.50 

of $SrCO_3$ and $CaCO_3$ as major surface contaminants after air exposure [10]. The build-up of contaminants on the XPS depthscale is rapid under ambient conditions, a contaminant layer of about 12 Å thick developing on the surface of $YBa_2Cu_3O_7$ ceramics after ~10 minutes air exposure [8].

Thus sample surfaces must be cleaned *in situ* before UHV electron spectroscopic measurements can begin. A particular problem with oxide superconductors is that they are usually prepared under highly oxidising conditions and may be susceptible to oxygen loss in UHV. Thus the usual cleaning procedure of argon ion bombardment and vacuum annealing is generally recognised to be unsuitable for cuprate superconductors, ultimately effecting a reduction of all the copper ions to a Cu(I) state [11]. The most popular alternative involves scraping or fracturing ceramic bars [12]. Whilst much high quality data have been obtained in this way there is a danger that this method will merely serve to expose contaminated grain boundaries or redistribute contamination on the sample surface [12, 13]. An attractive alternative is to peel, fracture or abrade single crystal samples. This approach has been applied to both $La_{2-x}Sr_xCuO_4$ [14, 15] and 123-type materials [16–21] although the availability of sufficiently large and well oxygenated samples is undoubtedly a problem for these compounds. Studies of single crystal $Bi_2Sr_2Ca_{n-1}Cu_nO_{4+2n}$ have been more widespread [22–36] and are facilitated by the ease with which these materials cleave *in vacuo*. In the case of $YBa_2Cu_3O_{7-x}$ and $EuBa_2Cu_3O_{7-x}$ it has been claimed that the single crystals must be cleaved at very low temperature (~20 K) to prevent oxygen loss [18–20]. This is a controversial point [21] to which we will return later.

Our own approach to sample cleaning involves reversing the effects of atmospheric degradation by *in situ* annealing under conditions chosen to mimic those used in the synthesis of the samples. Experiments are conducted in a two-chamber Escalab spectrometer (VG Scientific). Samples are mounted on platinum stubs using platinum clasp wires and transferred to the spectrometer preparation chamber, which is filled to 1 bar with pure oxygen. Samples are then subject to an annealing and slow cooling cycle, heating being effected by coupling radiofrequency power from a Radyne 150 kHz, 1.5 kW generator to the sample stub using a water-cooled coaxial feedthrough coil. The maximum temperature in the annealing cycle is somewhat below the firing temperature used in normal ceramic solid state syntheses. Typically in our own work we have used the following temperatures:

| | |
|---|---|
| $La_{2-x}Sr_xCuO_4$ | 800 °C |
| $YBa_2Cu_3O_{7-x}$ | 600–700 °C |
| $Bi_2(Sr, Ca)_3Cu_2O_8$ | 600 °C. |

Following periods of at least one hour at the maximum temperature, samples are slow cooled in an atmosphere of oxygen to around 400 °C to allow full oxygenation of the surface. The preparation chamber is then evacuated with the sequential aid of a molecular sieve-trapped rotary pump, a liquid nitrogen-trapped, polyphenyl ether-filled diffusion pump and a titanium sublimation pump to a base pressure of $<10^{-9}$ mbar. Samples are then transferred to the spectrometer main chamber (base pressure $5 \times 10^{-11}$ mbar). This is equipped with a 150 mm mean radius spherical sector analyser and has facilities for excitation of photoemission spectra with either a noble gas discharge lamp or soft x-rays from a Mg–Al twin anode gun.

The efficacy of the cleaning procedure may be gauged by monitoring the C : 1s/O : 1s intensity ratio. In the case of ceramic samples of $YBa_2Cu_3O_{7-x}$ the ratio may be reduced to below 1/100 [12], corresponding to residual hydrocarbon or carbonate coverages of at most $\frac{1}{4}$ monolayer. For $Bi_2Sr_2Ca_{n-1}Cu_nO_{4+2n}$ it is possible to reduce the C : 1s signal below levels of detectability [10, 37, 38]. Contaminated surfaces display a strong, high binding energy O : 1s component. This is chemically shifted by about 2–3 eV to higher binding energy of the O : 1s peak at 528–529 eV associated with the superconductor phase. The high binding energy peak shows enhanced intensity at shallow angle of offtake of photoelectrons (figure 1), thus demonstrating its surface origin. Even after complete removal of carbon we often see a sizable residual shoulder, presumably pointing to hydroxide or extraneous surface oxide phases. However, after judicious *in situ* oxygen annealing we have been able to reduce the high binding energy intensity to less than 1/10 of that of the main peak in the case of both $La_{2-x}Sr_xCuO_4$ (figure 1) and $Bi_2Sr_2Ca_{n-1}Cu_nO_{4+2n}$. It has been more difficult in our

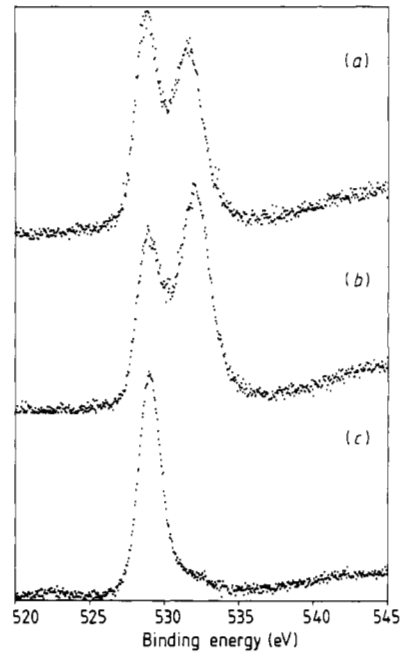


**Figure 1.** Al Kα XPS of $La_{1.85}Sr_{0.15}CuO_4$ in O : 1s region. (*a*) Normal emission spectrum of contaminated sample. (*b*) 15° emission (relative to surface plane) spectrum of contaminated sample. Note increase in intensity of high binding energy O : 1s component. (*c*) Normal emission spectrum of oxygen-annealed sample. Note low intensity of high binding energy O : 1s component.

experience to reduce the high binding energy peak to a similarly low level for $YBa_2Cu_3O_{7-x}$. The possibility that some of the residual O : 1s shoulder intensity is intrinsic to superconducting phases is discussed in section 3.

The low levels of contamination after *in situ* oxygen annealing match those achieved by cleavage or scraping of single crystals. However, our method of surface preparation offers the advantage that it can be applied to ceramic, bulk single crystals *and* polycrystalline or epitaxial single-crystal thin films. To date our work on thin films has been restricted to polycrystalline (but highly textured) Bi–Sr–Ca–Cu–O films [38], although Sakisaka *et al* have used an analogous oxygen annealing procedure to produce clean ordered (001) surfaces of $YBa_2Cu_3O_{7-x}$ epitaxial thin films [39, 40]. The oxygen-annealed surfaces are of immediate interest in relation to technological application of oxide superconductors, because they represent 'intrinsic' free surfaces of samples after furnace preparation and it is usually to these surfaces that contact must be made for electrical measurements. It should be recognised that there can be significant differences between cleavage surfaces and annealed external surfaces. Firstly the chemical composition of oxygen-annealed surfaces can differ from the bulk composition due to segregation, leading ultimately to formation of new 'surface phases'. In the case of $Bi_2(Sr, Ca)_3Cu_2O_4$ ceramics the surface composition derived by dividing XPS peak areas by elemental sensitivity factors is tolerably close to the bulk value [10]. By contrast, segregation effects are particularly striking for $La_{2-x}Sr_xCuO_4$. Here the Sr/La ratio of oxygen-annealed surfaces may be gauged by comparing intensities of La : 4d and Sr : 3d core level peaks (figure 2) which lie in the same energy region and have similar ionisation cross sections. The Sr/La ratio is consistently greater than expected from the bulk doping level (figure 3). Similar behaviour has recently been found at grain boundaries in this material by scanning Auger spectroscopy [41]. Analogous Sr enrichment is found in the related perovskite systems $La_{1-x}Sr_xVO_3$ [42] and $La_{1-x}Sr_xCoO_3$ [43] (figure 3) and is apparently driven by the fact that the ionic radius of the $Sr^{2+}$ dopant ($r$ = 1.28 Å) is larger than that of the host $La^{3+}$ ($r$ = 1.20 Å). The dopant ion produces less elastic strain when accommodated in surface, as opposed to bulk, sites. A second potential source of difference between the behaviour of oxygen-annealed and cleavage surfaces arises from different reactivity towards gases in the residual vacuum, particularly water vapour. It is well established that in the case of the perovskite $SrTiO_3$, the sticking coefficient for water on annealed surfaces is exceedingly low [44, 45]. By contrast on cleavage surfaces containing high step densities [45] or on surfaces in which defects are introduced by ion bombardment [44], the sticking coefficient is close to unity and surface $H_2O$ and $OH^-$ species rapidly accumulate upon exposure to the residual vacuum. The high reactivity of surfaces prepared by cleavage, fracture or abrasion may account for the observation of Takahashi and co-workers of rapid buildup of an O : 1s high binding energy shoulder on abraded $La_{2-x}Sr_xCuO_4$ single crystal surfaces [23] on holding samples in UHV. By contrast we have not found any marked deterioration of oxygen-annealed $La_{2-x}Sr_xCuO_4$ surfaces over a period of several hours [9].

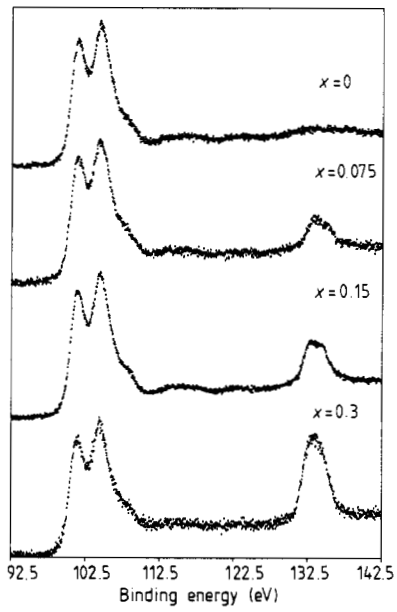


**Figure 2.** Normal emission Al Kα XPS of $La_{2-x}Sr_xCuO_4$ in La : 4d (102.5 eV) + Sr : 3d (132.5 eV) region as a function of Sr composition parameter $x$. Samples have been subject to *in situ* oxygen annealing. The La : 4d and Sr : 3d shells have similar photoionisation cross sections.

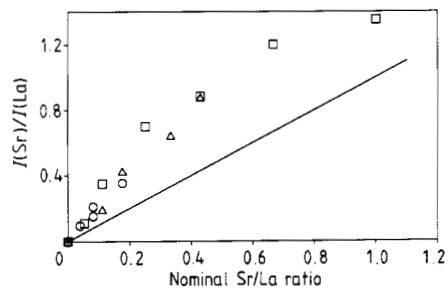


**Figure 3.** La : 4d to Sr : 3d XPS intensity ratio corrected for ionisation cross sections plotted against nominal Sr/La composition ratio for $La_{2-x}Sr_xCuO_4$ (circles, present work) $La_{1-x}Sr_xVO_3$ (triangles [42]) and $La_{1-x}Sr_xCoO_3$ (squares [43]). All data relate to *in situ* annealed samples. The full line shows the ratio expected in the absence of surface Sr segregation.

## 3. Core level studies

The major interest in core level photoemission lies in the ability of the technique to identify valence states of atoms in oxide superconductors by virtue of the chemical shift resulting from changing oxidation state. We confine the present discussion to Cu and O core levels,

which have been most widely studied using laboratory Mg K$\alpha$ ($h\nu$ = 1253.6 eV) and Al K$\alpha$ ($h\nu$ = 1486.6 eV) x-ray sources. The cuprate superconductors are dominantly Cu(II) compounds but extra holes are introduced into the valence bands by oxygen doping ($YBa_2Cu_3O_{7-x}$ with $x < 0.5$; possibly also $Bi_2Sr_{2-\delta}Ca_{n-1}Cu_nO_{4+2n+x}$); by countercation deficiency (possibly $Bi_2Sr_{2-\delta}Ca_{n-1}Cu_nO_{4+2n+x}$) or by substituting a countercation with a countercation of lower charge ($La_{2-x}Sr_xCuO_4$). The extra holes are formally accommodated by oxidation of Cu(II) ions to the Cu(III) state, although a major question is whether the holes might not be of dominant O : 2p character. In $La_{2-x}Sr_xCuO_4$ ($x < 0.5$), the formal Cu(III)/Cu(II) ratio is $x/(1-x)$, whilst in the 123 system $(1-2x)$ Cu(II) ions per cell are oxidised to Cu(III) for $x$ values less than 0.5. For $x$ values in the range $0.5 < x < 1$, $(x-0.5)$ Cu ions per cell are reduced to the Cu(I) state. Of course the metallic room temperature behaviour of the cuprate materials implies the holes are itinerant in the initial state. However, we expect the final state core-valence Coulombic interaction resulting from ionisation of copper core levels to be sufficiently strong to localise the Cu(I), Cu(II) and Cu(III) valence states. Thus Cu core level XPS should provide a direct means of interrogating holes in the valence band.

Interpretation of Cu core level data is complicated by strong Cu : 3d–O : 2p covalency resulting from near degeneracy of the respective atomic levels. Thus the Cu(II) initial state is a mixture of $Cu3d^9\underline{L}^0$ and $Cu3d^{10}\underline{L}^1$ configurations, where $\underline{L}$ denotes holes on the ligand oxygen ions (i.e. $\underline{L}^1$ is a single ligand hole configuration and $\underline{L}^0$ is a no ligand hole configuration). Likewise Cu(III) must be expressed as a mixture of $Cu3d^8\underline{L}^0$, $Cu3d^9\underline{L}^1$ and $Cu3d^{10}\underline{L}^2$. Cu(I) is simply $Cu3d^{10}\underline{L}^0$. Most copper core level work concentrates on the Cu : 2p level because of its high cross section for photoionisation by Al K$\alpha$ and Mg K$\alpha$ radiation. In Cu : 2p core level XPS we introduce a hole into the Cu $2p^6$ configuration so that possible final states are as follows:

| | |
|---|---|
| Cu(I) | $Cu2p^5Cu3d^{10}\underline{L}^0$ |
| Cu(II) | $Cu2p^5Cu3d^9\underline{L}^0$ |
| | $Cu2p^5Cu3d^{10}\underline{L}^1$ |
| Cu(III) | $Cu2p^5Cu3d^8\underline{L}^0$ |
| | $Cu2p^5Cu3d^9\underline{L}^1$ |
| | $Cu2p^5Cu3d^{10}\underline{L}^2$. |

Depending on their energy separation there can be mixing between the various 'pure' final state configurations. However, the mixing is less pronounced than in the initial state because the Coulomb interaction pulls the Cu : 3d states well below the O : 2p states. The relative intensities of the possible final state peaks thus reflect both initial state mixing and the magnitude of the core-valence Coulomb interaction.

Bearing these ideas in mind we turn to $Cu2p_{3/2}$ XPS data from $YBa_2Cu_3O_{7-x}$ ceramics [46]: a nominal $x$ value of 0 results from *in situ* oxygen annealing and an $x$ value of 1 from annealing at 600 °C for 16 hours in UHV. The spectral profile both before and after annealing is dominated by a peak between 930 eV and 935 eV and a broader, more structured and weaker peak between 940 and 947 eV (figure 4). The former arises from 'well screened' $Cu3d^{10}\underline{L}^n$ ($n$ = 0, 1 or 2) configurations and the latter from 'poorly screened' $Cu3d^9\underline{L}^n$ ($n$ = 1 or 2) states. In going from metallic (m) $YBa_2Cu_3O_7$ to non-metallic (n) $YBa_2Cu_3O_6$ we see a transfer in spectral weight from the high binding energy side of the well screened peak to the low binding energy side, together with an overall narrowing of the well screened peak. Note also the reduction in intensity of the $Cu3d^9$ satellite peak. Difference spectra (d) strongly suggest the expected shift from $Cu2p^5Cu3d^{10}\underline{L}^2$ final states at 935 eV to $Cu2p^5Cu3d^{10}\underline{L}^0$ final states at 932 eV as we go from $YBa_2Cu_3O_7$ to $YBa_2Cu_3O_6$ respectively. Similar data have been obtained by at least five other groups [47–51]. Thus there is now strong evidence that copper core level XPS is able to provide a measure of the valence band hole concentration. Note however that holes manifest themselves in terms of $Cu2p^5Cu3d^{10}\underline{L}^2$ final states and there have been no indications of $Cu2p^5Cu3d^8L^0$ final states that might naively be expected on the basis of $3d^8Cu^{3+}$ ions. (In fact it would be difficult to locate Cu : $2p_{3/2}$ structure due to the $Cu3d^8$ configuration because of overlap with the Cu : $2p_{1/2}$ peak.)

We turn now to other cuprate systems. Although there has been a claim of observation of a

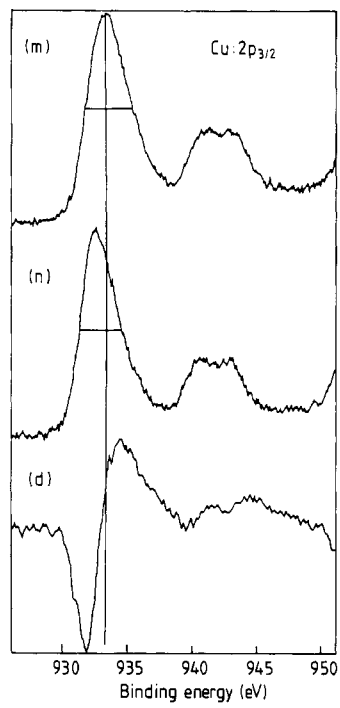


**Figure 4.** Normal emission Cu : $2p_{3/2}$ Al K$\alpha$ XPS of nominal metallic $YBa_2Cu_3O_7$(m) and non-metallic $YBa_2Cu_3O_6$ (n). The difference spectrum (d) obtained by subtracting (n) from (m) emphasises changes between the two. See text for details of sample preparation procedures. Adapted from [46].

$Cu2p^5Cu3d^{10}\underline{L}^2$ shoulder in XPS of $La_{1.85}Sr_{0.15}CuO_4$ [52], the data are not clearcut in demonstrating a build up of intensity as the hole concentration increases and further work is needed for this system [51]. For the $Bi_2Sr_2Ca_{n-1}Cu_nO_{4+2n}$ system the ability to control the hole concentration is less well developed and there is as yet no data showing well defined changes in Cu : 2p spectra as a function of changes in hole concentration.

Moving on to O : 1s core structure, we consider first possible final state configurations. At the outset, it must be recognised that the O : 1s–O : 2p core valence Coulomb interaction may be insufficient to localise the final states owing to the relatively large O : 2p bandwidth [27]. An additional complication is that there are in general inequivalent O sites with not all of the O atoms bonded to copper. However, the chemical shifts between different sites within the superconducting phases will be rather small and at most will produce broadening of the main O : 1s peak. Adopting a localised description, we have the following final state configurations for O atoms bonded to copper:

| | |
|---|---|
| Cu(I) | $O1s^1Cu3d^{10}\underline{L}^0$ |
| Cu(II) | $O1s^1Cu3d^9\underline{L}^0$ |
| | $O1s^1Cu3d^{10}\underline{L}^1$ |
| Cu(III) | $O1s^1Cu3d^8\underline{L}^0$ |
| | $O1s^1Cu3d^9\underline{L}^1$ |
| | $O1s^1Cu3d^{10}\underline{L}^2$. |

Satellite structures in XPS of CuO appearing 1.5 eV to higher binding energy of the main peak has been interpreted in terms of poorly screened (i.e. with incomplete O : 2p valence levels) $O1s^1Cu3d^{10}\underline{L}^1$ final states [53] although an alternative explanation is given in terms of contaminants [54]. Analogous structure in XPS of $RE_2CuO_4$ (RE = rare earth), $YBa_2Cu_3O_7$ [53] and $Bi_2Sr_2CaCu_2O_8$ [25], appearing between the main O : 1s core peak and the contaminant peak, has been discussed in terms of the two intrinsic O : 1s hole states for Cu(II). There must be strong mixing between the two final state configurations and the distinction between well screened (dominant $O1s^1Cu3d^9\underline{L}^0$) and poorly screened (dominant $O1s^1Cu3d^{10}\underline{L}^1$) final states depends critically on initial state atomic eigenvalues and core–valence Coulomb interactions.

Holes in oxygen valence band states should allow observation of further final states, the configuration $O1s^1Cu3d^9\underline{L}^1$ arising from a one-electron process in which a core electron is removed from $O^-$. There are many pitfalls in interpretation of experimental O : 1s lineshapes arising from problems associated with surface contamination. It is beyond the scope of this paper to reference innumerable papers dealing with O : 1s lineshapes for heavily contaminated samples, i.e. those where the high binding energy O : 1s peak has an intensity comparable with or greater than that of the 529 eV peak. Nonetheless it should be recognised that *weak* high binding energy structure may be intrinsic to cuprate phases and should increase in intensity with increasing concentrations of holes in the valence bands. In our own work we believe that the greater O : 1s satellite intensity in XPS of Pb-stabilised $Bi_2Sr_2Ca_2Cu_3O_{10}$ as compared with $Bi_2Sr_2CaCu_2O_8$ in part reflects a greater hole concentration in the former material [37].

Goodenough and co-workers have introduced the further idea that in materials where direct O–O interactions are possible within the Cu(I) planes of the $YBa_2Cu_3O_7$ structure, O : 2p holes may be trapped out by formation of $O_2^{2-}$. An O : 1s component appearing between the main peak and the contaminant peak in XPS of compounds such as tetragonal semiconducting $YBa_2Cu_3O_{6.7}$, tetragonal metallic $YLa_{0.4}Ba_{1.6}Cu_3O_{7.05}$, and tetragonal semiconducting $La_{1.5}Ba_{1.5}Cu_3O_{7.19}$ is assigned to these peroxide species [55].

## 4. Valence region structure

Valence region photoemission provides a direct means of investigating the filled electronic states in oxide superconductors. Both tunable synchroton radiation and radiation from conventional noble gas discharge lamps or soft x-ray guns can be used to excite valence band spectra. Changes in intensity of spectral features with changing photon energy reflect changes in atomic ionisation cross sections and are of value in helping to identify the atomic nature of states responsible for valence band emission. Resonant enhancement of valence orbital cross sections at core excitation thresholds provides a particularly powerful approach here, although of course it usually demands use of synchroton radiation. Particular interest focuses on the nature of satellite structure in valence region photoemission (which is ultimately related to electron correlation), and on electronic states close to the Fermi energy. These topics are considered in sections 4.2 and 4.3 after a brief discussion of the gross features of the valence region photoemission structure in section 4.1.

### 4.1. Gross features of valence band structure

He(I) ($h\nu$ = 21.2 eV) UPS of oxygen-annealed polycrystalline $La_{1.85}Sr_{0.15}CuO_4$, $YBa_2Cu_3O_7$, $Bi_2(Sr,Ca)_3CuO_8$ and Pb-stabilised $Bi_2Ca_2Sr_2Cu_3O_{10}$ are shown in figure 5. The spectral range in these data is limited by a strong background of secondary emission features beyond 10 eV apparent binding energy. Spectra excited with He(II) radiation ($h\nu$ = 40.8 eV) extend to higher binding energy and allow the observation of satellite structure below the main valence band peak (figure 6) and of shallow core levels. The overall band profiles are for the most part in agreement with data from cleaved, scraped or fractured surfaces. This shows that the valence band density of states supported by the oxygen-annealed surfaces does not in general differ markedly from the density of states probed on surfaces prepared by other means. The density of states at the

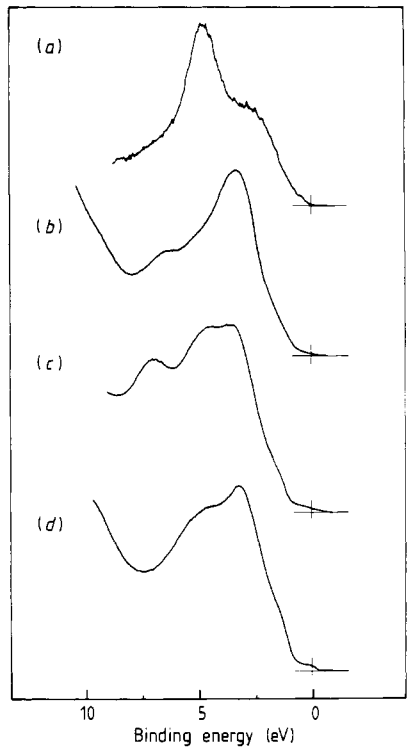


**Figure 5.** He(I) ($h\nu$ = 21.2 eV) photoemission spectra of oxygen-annealed ceramic cuprates: (*a*) $YBa_2Cu_3O_7$; (*b*) $La_{1.85}Sr_{0.15}CuO_4$; (*c*) $Bi_2Sr_{1.5}Ca_{1.5}Cu_2O_8$; (*d*) Pb-stabilised $Bi_2Sr_2Ca_2Cu_3O_{10}$. All spectra were recorded at room temperature in normal emission.

Fermi energy (manifest in terms of a characteristic sharp cut-off in He(I) photoemission spectra) increases with increasing $T_c$ in the series $La_{1.85}Sr_{0.15}CuO_4$ < $Bi_2(Sr,Ca)_3Cu_2O_8$ < Pb-stabilised $Bi_2Sr_2Ca_3Cu_3O_8$. However, the density of states at $E_F$ is anomalously low

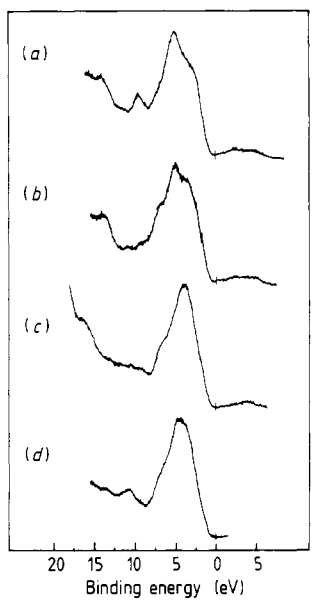


**Figure 6.** He(II) ($h\nu$ = 40.8 eV) photoemission spectra of oxygen-annealed ceramic cuprates: (*a*) $YBa_2Cu_3O_7$; (*b*) $YBa_2Cu_3O_6$; (*c*) $La_{1.85}Sr_{0.15}CuO_4$; (*d*) $Bi_2Sr_{1.5}Ca_{1.5}Cu_2O_8$. All spectra were recorded at room temperature in normal emission. Structure apparently above the Fermi energy is excited with satellite He(II) $\beta$ radiation ($h\nu$ = 48.4 eV).

for $YBa_2Cu_3O_7$. Whilst this latter observation is in agreement with most other published data, considerable controversy now surrounds photoemission data for this compound. In particular Arko *et al* [20] have recently reported photoemission spectra from two single crystals cleaved at 20 K. For both cleaves there is a large density of states at the Fermi energy. Whilst the overall bandshape for one cleave is similar to that in figure 6, the shape for the other cleave is radically different, with the maximum photoemission intensity not at 4.8 eV but at about 2.0 eV.

The first comment in relation to the photoemission profiles is that they are very different from those for d" perovskites containing transition elements from earlier in the transition series. For compounds such as $LaVO_3$ [42], $Na_xWO_3$ [56] and $SrRuO_3$ [57] it is possible to distinguish well separated O : 2p and M : nd bands, the latter lying at lower binding energy. Thus the data from cuprate superconductors immediately imply that Cu : 3d and O : 2p states are of comparable energy and that there must be extensive mixing between them. This extensive Cu : 3d/O : 2p hybridisation is a feature in most band-structure calculations (for an excellent review see [58]). However, to align observed photoemission profiles with calculated density-of-states profiles it is usually necessary to introduce a rigid downward shift of the complete band structure by an energy of order 1–2 eV. The shift is usually attributed to the effects of correlation, although it is surprising that both O : 2p and Cu : 3d structure must be shifted by the same energy [20, 58]. Arko *et al* have argued that the large shifts are an artefact of poor sample preparation, at least in the case of $YBa_2Cu_3O_7$ [20].

Where well defined peaks and shoulders are found within the overall band profile it is possible to make inferences about the dominant atomic parentage of states from changes in relative intensity with varying photon energy. Thus in the case of $YBa_2Cu_3O_7$, the He(I) profile has a strong central peak at 4.8 eV with shoulders at 2.6 eV and 7.0 eV. Upon increasing the photon energy (figure 7), the central peak decreases in intensity relative to the two shoulders. Similar behaviour is found in synchrotron radiation studies [39, 40, 59]. The O : 2p/Cu : 3d cross section ratio decreases with increasing photon energy, thus suggesting that the central peak relates to states of dominant O : 2p atomic character. Under Al K$\alpha$ x-ray photon excitation the O : 2p/Cu : 3d cross section ratio is only 0.08, so that valence region XPS essentially probes only the Cu : 3d partial density of states. The top spectrum of figure 7 thus implies that Cu : 3d character is spread across the complete width of the valence band. Note, however, that the measurements of Arko and co-workers [20] call into question whether these conclusions apply to $YBa_2Cu_3O_7$ or a phase of lower oxygen content.

### 4.2. Satellite structure

The photoemission structure appearing at binding energies below 8 eV for transition metal oxides toward the

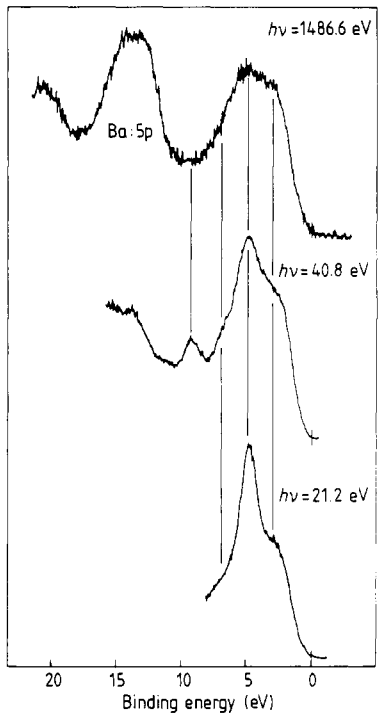


**Figure 7.** Photoemission spectra of $YBa_2Cu_3O_7$ at different photon energies.

right-hand side of the Periodic Table relates to final states where the photohole is screened by transfer of electron density from surrounding atoms. In ionisation of localised d electrons, the nominal d electron count in the excitonic final state is thus the same as that in the initial state due to charge transfer from surrounding ligand atoms. However, for these highly correlated systems, satellite structure corresponding to unscreened final states is expected at higher binding energy, the energy shift arising from strong onsite Coulomb interactions. Thus in the case of NiO ($Ni^{2+}$, configuration $3d^8$), ionisation of Ni : 3d electrons gives an unscreened Ni : $3d^7$ satellite at around 10 eV binding energy, the screened 3d peak (Ni : $3d^8\underline{L}^1$) being centred at 2 eV. The 8 eV shift reflects the large 3d–3d Coulomb repulsion [60, 61]. In the case of CuO ($Cu^{2+}$, configuration $3d^9$), the Cu : $3d^8$ satellites appear 10.5 eV and 12.9 eV below $E_F$, the latter peak being dominant. The CuO satellites show strong resonant enhancement at photon energies around the Cu : 3p core excitation threshold at $h\nu = 75$ eV. Interestingly, at this energy the main screened Cu : 3d structure shows antiresonance intensity variations [62]. Comparable satellite structure and resonance behaviour is therefore to be expected in photoemission of cuprate superconductors provided that correlation effects in these materials are comparable to those in CuO.

Satellite structure is most easily seen in photoemission data from the $La_{2-x}Sr_xCuO_4$ system because there is no overlap with shallow core level peaks. In $La_{1.8}Sr_{0.2}CuO_4$ a resonantly enhanced satellite appears at 12.3 eV [63]. For $YBa_2Cu_3O_7$ problems arise in observing Cu satellites at resonant photon energies using synchrotron radiation because of interference from Ba : 4d structure excited with second-order radiation. There is also some interference from the Ba : $5p_{3/2}$ level. However, with due attention to interference from the Ba peaks, a well defined copper satellite showing resonance enhancement at $h\nu = 74$ eV is found at 12.3–12.9 eV [17, 20, 40, 63–68] in synchrotron radiation-excited data taken from both single-crystal and polycrystalline samples. For $Bi_2Sr_2CaCu_2O_8$ there is again a problem with overlap with structure due to counter cations [25]. This arises from the Bi : 6s orbitals which probably mix strongly with O : 2p states [33]. A broad band between 9 eV and 14 eV contains contributions from both copper satellites and the Bi : 6s levels. Resonant enhancement is observed in this region at the copper 3p threshold [23, 34, 69, 70], although Spicer and co-workers have shown that the enhancement in spectral weight is centred around 12.3 eV [69, 70]. Thus structure at lower binding energy within the band probably relates to Bi : 6s states. Owing to the low cross section for ionisation of pure 6s electrons with vacuum UV radiation, most of the 6s intensity at low photon energies may come from mixing with O : 2p states. In summary then, the occurrence of satellite structure in photoemission from cuprate superconductors analogous to the 12.9 eV satellite of CuO is relatively uncontroversial.

The presence of *additional* satellite structure has proved to be perhaps the most contentious issue in photoemission studies of oxide superconductors. The observation of two satellite peaks in CuO photoemission is due to multiplet splitting within the Cu : $3d^8$ configuration and it should be recognised at the outset that similar multiplet splitting may prevail in cuprate superconductors. Several other mechanisms for extra satellites may be envisaged [71]. For example it has been suggested by Ramaker [72] that Cu : 3d–O : 2p covalency should allow the possibility of $3d^{10}\underline{LL}$ final states in valence region photoemission. The $\underline{LL}$ notation here implies the existence of two holes within the O : 2p valence states, but the two holes are located on different oxygen atoms within the $CuO_n$ coordination polyhedron; where two holes are on the same site we use the $\underline{L}^2$ notation. If the holes are on ortho-oxygen atoms one can envisage the formation of bonding and antibonding $\underline{LL}$ states. The lower (bonding) combination is predicted to lie at 9.5 eV binding energy, well below the main valence band peak. An $\underline{L}^2$ satellite with two holes on the same oxygen ion was also considered in this work, but owing to the larger value of the on-site Coulomb interaction as compared with the intrasite Coulomb interaction, the energy was predicted to be 15 eV below $E_F$. Kurtz *et al* have argued that the $3d^{10}\underline{LL}$ final state should show resonant enhancement at the O : 2s threshold [73]. Introduction of holes into the initial state of the system leads to other possible final states which may be designated as $Cu3d^7$, $Cu3d^9\underline{L}^2$, $Cu3d^9\underline{LL}$, $Cu3d^{10}\underline{L}^3$, $Cu3d^{10}\underline{L}^2\underline{L}$, $Cu3d^{10}\underline{LLL}$ etc. Kurtz *et al* have argued that the presence of three ligand holes in the

Cu3d$^{10}$LLL configuration will 'quench' the appearance of 3d$^{10}$LL satellite structure.

Early experimental work appeared to confirm the existence of extra satellite structure. Thus in nearly all experiments on polycrystalline metallic $YBa_2Cu_3O_7$ a well defined peak was observed at 9.5 eV binding energy. Our own results (figure 6) are typical in this respect. Experimental work from two groups [59, 65] suggested that the 9.5 eV satellite was resonantly enhanced at the Cu : 2p core threshold as expected for a Cu : 3d$^7$ or Cu : 3d$^8$ satellite. However, this result has not been confirmed elsewhere [15, 17, 64, 66]. Indeed at lower photon energies Kurtz and co-workers found resonant enhancement at the O : 2s threshold [73] favouring assignment in terms of 3d$^{10}$LL final states.

Widespread speculation [11–13, 53, 59, 63] that surface contaminants could produce photoemission structure in the 9.5 eV satellite region receives support from adsorption experiments on polycrystalline $YBa_2Cu_3O_{7-x}$ [74] and $La_{2-x}Sr_xCuO_4$ [75]. Thus Johnson and co-workers [74] demonstrated that photoemission intensity in the region of the 9.5 eV satellite increased upon allowing a surface on which water had been condensed at 20 K to warm to room temperature. A parallel increase in intensity of the high binding energy O : 1s component was found. Likewise for $La_{1.8}Sr_{0.2}CuO_4$, Madey and co-workers found a buildup of intensity just below the main valence band upon exposure of a scraped ceramic to water vapour at room temperature, with an apparent sticking coefficient close to unity [75]. This latter work established that the $\sigma$ level of hydroxyl groups coincides almost exactly with 9.5 eV 'satellite' structure for the unexposed sample, as might have been expected from earlier chemisorption studies on $SrTiO_3$ [44, 45]. Note however that the initial 'satellite' intensity in the experiments of Madey and co-workers is very much stronger than in our own work on oxygen-annealed polycrystalline samples (figure 7) suggesting that the initial reference surface was somewhat contaminated. Nonetheless, the adsorption experiments do not exclude the possibility that *some* of the intensity around 9.5 eV may be intrinsic to superconducting phases. Similarly, the observation [46, 47, 76, see also figure 6] that the 9.5 eV satellite largely vanishes, upon vacuum-annealing nominal $YBa_2Cu_3O_7$ to effect a transformation to $YBa_2Cu_3O_6$, does not distinguish between the possibilities that the changes result from the desorption of a contaminant species ($OH^-$), or that the transformation quenches satellite structure intrinsic to the highly oxygenated phase.

Unfortunately work on single crystal samples does not completely resolve the controversies surrounding the 9.5 eV satellite. Interpretation of data from $Bi_2Sr_2CaCu_2O_8$ samples suffers from the problem of intrinsic Bi : 6s related emission so that our discussion will be restricted to $La_{2-x}Sr_xCuO_4$ and $YBa_2Cu_3O_{7-x}$. In the first experiments [17] on single crystal $YBa_2Cu_3O_7$, a strong peak at 9.5 eV was found for at least ten different cleavage surfaces, including some where cleavage was carried out at 77 K. The satellite showed no Cu : 3p resonance behaviour and was interpreted in terms of Wendin's two oxygen hole model [71]. By contrast for $La_{2-x}Sr_xCuO_4$ ($x = 0$ and 0.04) Takahashi *et al* [14] found that scraped, single-crystal surfaces held at low temperatures ($< 150$ K) gave very low satellite intensity but on warming to room temperature a peak at 10 eV in He(II) photoemission ($h\nu = 40.8$ eV) grew rapidly. Similar behaviour is found in the experiments of Arko *et al* on cleaved $EuBa_2Cu_3O_{7-x}$ [18, 19] and $YBa_2Cu_3O_{7-x}$ [20]. For the Y compound, the 9.5 eV satellite is absent on data taken from crystals with $x$ values close to 0.1 and 0.75 cleaved at 20 K, but grows rapidly as the crystal is allowed to warm to room temperature. Note that in this work a weak but resonantly enhanced copper satellite is found at 10 eV, as expected from the experiments on CuO (see above). The time-dependent behaviour leads to the interesting suggestion that the 9.5 eV satellite is associated with adsorbed oxygen or interstitial oxygen. These oxygen species derive in turn from the decomposing bulk crystal. Alternatively Kurtz and co-workers [73] have argued that the 9.5 eV satellite is intrinsic to $x$ values around 0.5 and is absent if there is significant oxidation or reduction to either Cu(III) or Cu(I). This latter suggestion is difficult to reconcile with the absence of satellite structure [14] for $La_2CuO_4$ (a Cu(II) compound) and with the growth of satellite intensity resulting from degradation of $YBa_2Cu_3O_{6.25}$. On the other hand, the explanation in terms of oxygen loss and readsorption provides no obvious rationale of the observation [20] of more rapid growth of satellite structure in crystals with large $x$ value (low oxygen content), as compared with crystals of low $x$ value (high oxygen content). Contrasting with the experimental work on cleavage surfaces, Sakisaka *et al* [39, 40] find no time-dependent growth of 9.5 eV satellite structure in photoemission from oxygen-annealed, single crystal thin films of $YBa_2Cu_3O_7$ [39, 40]. However, a peak is observed at 8.5 eV for photon energies close to 40 eV. This is attributed to the bottom bands of the one-electron band structure, which reach their lowest energy at the M point of the Brillouin zone.

Thus there is at present no clear consensus regarding 9.5 eV satellite structure in photoemission from cuprate superconductors, although it is difficult to avoid the conclusion that it relates at least in part to surface contamination, probably by hydroxyl groups. The higher sticking coefficient of water on oxide cleavage surfaces as compared with oxygen-annealed surfaces should be more widely recognised and further careful surface experiments are needed using techniques which can distinguish unambiguously between adsorbed carbonate, hydroxide and oxygen. Application of high resolution electron energy loss spectroscopy (HREELS) to provide a vibrational fingerprint of the surface would be particularly valuable in this respect. Unfortunately intrinsic surface phonon structure provides a strong background in HREELS from oxides [77], and existing HREELS data [78–80] are of too poor a quality to reveal vibrational features due to adsorbates.

### 4.3. Fermi energy structure in photoemission

The transition of cuprate materials from a normal metallic into a superconducting state depends ultimately on the behaviour of electrons close to the Fermi energy ($E_F$) in the normal state. Thus there has been a great deal of interest in Fermi level structure in photoemission, and changes therein, on going into a superconducting state. Any changes in photoemission spectra will take place on an energy scale of order $kT_c$, which is of course at least a factor of two lower for $La_{1.85}Sr_{0.15}CuO_4$ than for $YBa_2Cu_3O_7$ and $Bi_2Sr_2CaCu_2O_8$. Although well defined metallic Fermi edges can be seen in photoemission from $La_{2-x}Sr_xO_4$ [63, 81, see also figure 5] most interest has centred on the compounds with the higher transition temperatures and we confine our discussion to them.

Despite two reports of a Fermi edge cut-off in photoemission from $YBa_2Cu_3O_7$ [82, 83] a consensus arose during 1987–1988 that the density of states at the Fermi energy in room temperature photoemission was below the levels of detectability. This puzzling result is at variance with band-structure calculations which uniformly predict a density of states at $E_F$ ($g(E_F)$) of order 2–3 states/eV cell [58]. Although the photoemission data could be taken to indicate that the normal state of $YBa_2Cu_3O_7$ does not behave like a Fermi liquid, more plausible explanations can be couched in terms of surface effects. Thus oxygen loss from the surface region can lead to a lowering of oxygen stoichiometry below $O_{6.5}$ and a transformation to a non-metallic state. Alternatively there is the possibility of intrinsic hole localisation due to band narrowing at the surface of metallic $YBa_2Cu_3O_7$ [84]. The experimental situation changed dramatically with the work on low-temperature cleaved $EuBa_2Cu_3O_7$ [18, 19] and $YBa_2Cu_3O_7$ [20] discussed earlier. Here a density of states at $E_F$ of the order of 20% of that of metallic copper was found after 20 K cleavage. From intensity variation with varying photon energy the states at $E_F$ were estimated to be of 80% O : 2p and 20% Cu : 3d character. As the temperature of the cleaved surface was raised above 50 K the density of states at $E_F$ declined progressively and irreversibly, reaching zero at room temperature. This appears to support the oxygen loss hypothesis although it is hard to reconcile the valence photoemission data with core level data pointing clearly to the existence of valence band holes, which can only arise from oxygen stoichiometry in excess of $O_{6.5}$ (section 3). The experimental observations of Arko *et al* have not been confirmed by other groups and indeed very recently Brundle and co-workers have observed a high density of states at $E_F$ in room-temperature cleaved $YBa_2Cu_3O_7$ [21]. In this work the Fermi structure shows no change with time at room temperature. The experimental situation is further complicated by the observation by Sakisaka *et al* of a small but stable Fermi edge discontinuity at restricted $k$ values in angle-resolved photoemission data from epitaxial, oxygen-annealed $YBa_2Cu_3O_7$ films [39, 40]. The overall valence band profiles in this work more closely resemble the previous 'consensus' bandshape than in the experiments of Arko *et al*. Clearly more work is needed to clarify the relationship between the density of states at $E_F$ and surface oxygen content and to identify factors influencing UHV stability of $YBa_2Cu_3O_7$.

The situation with respect to Fermi level structure in photoemission from $Bi_2Sr_2CaCu_2O_8$ has proved to be less controversial. Our own finding [10, 37, 38, see also figure 5] of a small but well defined density of states at $E_F$ in spectra of oxygen-annealed $Bi_2(Sr, Ca)_3Cu_2O_8$ is in broad agreement with measurements on both cleaved single crystal [22, 23, 25, 27–29, 31, 33–35] and abraded polycrystalline samples [22, 69, 70, 85–87]. Of course work on single crystals allows more detailed comparison with band-structure calculations and the study of dispersion in bands close to $E_F$ [23, 34]. The height of the Fermi edge discontinuity in He(I) ($h\nu = 21.2$ eV) photoemission from polycrystalline samples of $Bi_2Sr_2CaCu_2O_8$ is about 2% of the intensity of the valence band maximum [10, 22, 37, 38, 85]. Interpreting our own data [38] in terms of a very simple model that ignores variation in ionisation matrix elements and densities of accessible final states across the occupied valence band [56], the height of the Fermi edge discontinuity implies that the cut-off in the density of states is about 0.3 states/eV cell for the $Bi_2Sr_2CaCu_2O_8$ phase ($T_c = 80$ K) and 0.5 states/eV cell for the Pb-stabilised $Bi_2Sr_2Ca_2Cu_3O_{10}$ phase ($T_c = 110$ K). This appears to confirm the correlation between $T_c$ and $g(E_F)$ expected from BCS theory. However, the value of $g(E_F)$ for the 2212 phase is about a factor of ten lower than in most band-structure calculations [58].

Turning now to the atomic nature of the states at $E_F$, Takahashi *et al* claimed to observe resonant enhancement at $h\nu = 18$ eV, which was believed to lie close to the O : 2s threshold, but no resonant enhancement at the Cu : 3p threshold around $h\nu = 74$ eV thus confirming the dominant O : 2p nature of the states [23]. However, it has been argued that the 18 eV enhancement does not represent true O : 2s threshold resonance behaviour [20, 31] and that the lack of resonance at $h\nu = 74$ eV does not in itself establish that states have no Cu : 3d character. This latter assertion is based on the fact that the main valence band-structure, which must represent the primary d ionisation from the Cu : $3d^9$ configuration, itself shows only weak anti-resonance behaviour [20]. Nonetheless the states 0.5 eV below the Fermi energy in $Bi_2Sr_2Ca_{n-1}Cu_nO_{4+2n}$ ($n = 1$ or 2) seem to have appreciably less Cu : 3d character than corresponding states in $YBa_2Cu_3O_7$ and $La_{1.85}Sr_{0.15}CuO_4$, both of which show weak Cu : 3d resonant enhancement [70].

There has been some speculation that the ability to see Fermi edge structure in photoemission from $Bi_2Sr_2Ca_{n-1}Cu_nO_{4+2n}$ reflects metallicity of the Bi–O planes [29, 33, 37, 69, 86]. This idea receives support from the observation of a distinctly asymmetric Bi : 4f lineshape in core level XPS [29, 33, 37, 69, 85]. The asymmetry can be interpreted in terms of Doniach–

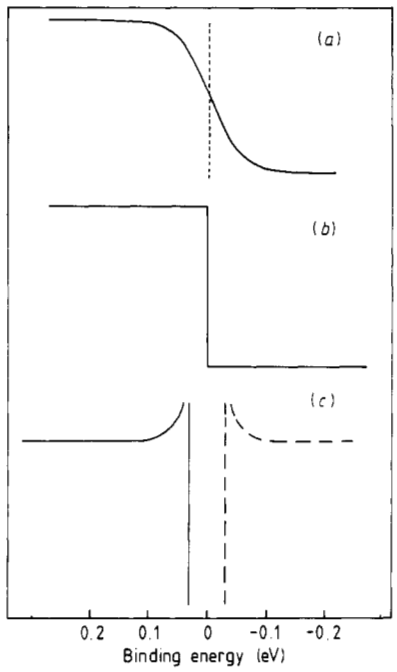


**Figure 8.** Schematic bandshapes in photoemission spectra: (*a*) normal metal at 300 K; (*b*) normal metal at 0 K; (*c*) superconductor at 0 K assuming BCS-like gap with $\Delta = 30$ meV. Broadening effects due to limited experimental resolution are not included. In (*c*) empty states that could be seen in inverse photoemission are shown by the broken curve.

Sunjic theory [88], implying in turn a significant Bi : 6s or Bi : 6p partial density of states at the Fermi energy. Interestingly, even larger Pb : 4f asymmetry in core level data from Pb-stabilised $Bi_2Sr_2Ca_2Cu_3O_{10}$ suggests both incorporation of Pb into the metallic 2223 phase and an even larger Pb contribution to states at $E_F$ [37]. These ideas are somewhat controversial and the Bi lineshape at least can be interpreted alternatively in terms of chemically shifted $Bi^{3+}$ and $Bi^{5+}$ components [29, 33]. The idea of metallic Bi–O planes has recently been called into question by Takahashi and co-workers [89] and by Shih *et al* [30] who used scanning tunnelling microscopy to examine $Bi_2Sr_2Ca_2Cu_3O_{10}$ cleavage surfaces. Use of the microscope in the topographic mode confirms that cleavage preferentially exposes Bi–O planes. In the spectroscopic mode an energy gap appears around $E_F$ in the normal state, suggesting that the Bi–O planes in the outermost atomic layer are non-metallic.

Undoubtedly the most spectacular result to have emerged from photoemission work on $Bi_2Sr_2CaCu_2O_8$ has been the observation of changes in structure close to the Fermi energy upon cooling the sample surface below the superconducting transition temperature. Provided the experimental resolution remains comparable to $kT$, one expects in the case of a normal metal merely to see a sharpening of the Fermi edge, in accordance with the Fermi–Dirac distribution function [90]. However, in a BCS-like superconducting state an energy gap in the quasiparticle density of states opens around $E_F$ and in photoemission one expects spectral weight to be pulled below the Fermi energy as shown schematically in figure 8. Spectral profiles conforming to this picture have now been observed by four groups [28, 31, 36, 91]. The data may be interpreted consistently in terms of an energy gap $\Delta = 30$ meV. This corresponds to $2\Delta(0)/k_BT_c \approx 8$, which is a factor of two larger than the weak coupling value of BCS theory. Considerable uncertainties surround measurements of the energy gap by other techniques such as tunnelling [92] and infrared spectroscopy. In particular Bonn *et al* [93] have asserted that, in the case of $YBa_2Cu_3O_7$ at least, no information about the gap can be inferred from infrared data because reflectance spectra are dominated by a plasma edge at 60 meV. Against this background the photoemission results are of special importance and extension of work on $Bi_2Sr_2CaCu_2O_8$ to other systems is a matter of some urgency.

## Acknowledgments

We are grateful for invaluable assistance from Dr D Geeson, Mr P C Hollamby and Mr J Hampson in our experimental programme. We also thank Professor D Tilley, Mr C Neeson, Dr S J Golden and Dr S E Male for the provision of samples. WRF thanks the Royal Society for the award of a 1983 University Research Fellowship and MG thanks ICI for the award of a CASE studentship. The research was supported by the SERC.

## References

[1] Bednorz J G and Müller K A 1986 *Z. Phys.* B **64** 189
[2] Tarascon J M, Greene L H, McKinnon W R, Hull G W and Geballe T H 1987 *Science* **235** 1373
[3] Jorgensen J D 1987 *Japan. J. Appl. Phys.* **26** (suppl. 26-3) 2017
[4] Maeda H, Tanaka M, Fukutomi M and Asano T 1988 *Japan. J. Appl. Phys. Lett.* **4** L209
[5] Sheng Z Z, Hermann A M, El Ali A, Almasan C, Estrada J, Datta T and Matson R J 1988 *Phys. Rev. Lett.* **60** 937
[6] Wonltungton T R, Gallagher W J and Dinger T R 1987 *Phys. Rev. Lett.* **59** 1160
[7] Yan M F, Barns R L, O'Bryan Jr H M, Gallagher P K, Sherwood R C and Jin S 1987 *Appl. Phys. Lett.* **51** 532
[8] Egdell R G, Flavell W R and Hollamby P C 1989 *J. Solid State Chem.* **79** 238
[9] Golden M S 1989 unpublished
[10] Flavell W R, Hampson J A, Neeson C and Tilley R J D 1989 *Supercond. Sci. Technol.* **1** 221
[11] Meyer III H M, Hill D M, Wagener T J, Gao Y, Weaver J H, Capone II D W and Goretta K C 1988 *Phys. Rev.* B **38** 6500
[12] Flavell W R and Egdell R G 1988 *Supercond. Sci. Technol.* **1** 118
[13] Yarmoff J A, Clarke D R, Drube W, Karlsson U O, Taleb-Ibrahimi A and Himpel F J 1987 *Phys. Rev.* B **36** 3967

[14] Takahashi T, Maeda F, Katayama-Yoshida H, Okabe Y, Suzuki T, Fujimori A, Hosoya S, Shamoto S and Sato M 1988 *Phys. Rev.* B **37** 9788
[15] Brookes N, Viescas A, Johnson P D, Remeika J P, Cooper A S and Smith N V 1988 *Surf. Sci.* **203** L627
[16] Stoffel N G, Cang Y, Kelly M K, Dottl L, Onellion M, Morris P A, Bonner W A and Margaritondo G 1988 *Phys. Rev.* B **37** 7952
[17] Ming Tang, Stoffel N G, Qi Biao Chen, LaGraffe D, Morris P A, Bonner W A, Margaritondo G and Onellion M 1988 *Phys. Rev.* B **38** 897
[18] Arko A J *et al* 1988 *J. Magn. Magn. Mater.* **75** L1
[19] List R S *et al* 1988 *Phys. Rev.* B **38** 11966
[20] Arko A J *et al* 1989 *Phys. Rev.* B **40** 2268
[21] Fowler D E, Lerczak J, Brundle C R and Holizberg R 1989 *Int. Meeting on High Temperature Superconductivity (Stanford) July 1989* (Abstract 5B-24)
[22] Onellion M, Ming Tang, Chang Y, Margaritondo G, Tarascon J M, Morris P A, Bonner W A and Stoffel N G 1988 *Phys. Rev.* B **38** 881
[23] Takahashi T, Matsuyama H, Katayama-Yoshida H, Okabe Y, Hosoya S, Seki K, Fujimoto H, Sato M and Inokuchi H 1988 *Nature* **334** 691
[24] Kohiki S, Wada T, Kawashima S, Takagi H, Uchida S and Tanaka S 1988 *Phys. Rev.* B **38** 7051
[25] Meyer H M III, Hill D M, Weaver J H, Nelson D L and Gallo C F 1988 *Phys. Rev.* B **38** 7144
[26] Himpsel F J, Chandrashekhar G V, McLean A B and Shafer M W 1988 *Phys. Rev.* B **38** 11946
[27] Shen Z-X, Lindberg P A P, Wells B O, Mitzi D B, Lindau I, Spicer W E and Kapitulnik A 1988 *Phys. Rev.* B **38** 11820
[28] Imer J-M, Patthey F, Dardel B, Schneider W-D, Baer Y, Petroff Y and Zettl A 1989 *Phys. Rev. Lett.* **62** 336
[29] Hillebrecht F U *et al* 1989 *Phys. Rev.* B **39** 236
[30] Shih C K, Feenstra R M, Kirtley J R and Chandrashekhar G V 1989 *Phys. Rev.* B **40** 2682
[31] Manzke R, Buslaps T, Claessen and Fink J 1989 *Europhys. Lett.* in the press
[32] Claessen R, Manzke H, Cartensen B, Burandy B, Buslaps T, Skibowski M and Fink J 1989 *Phys. Rev.* B **39** 7316
[33] Fujimori A, Takekawa S, Takayama-Muromachi E, Uchida Y, Ono A, Takahashi T, Okabe Y and Katayama-Yoshida H 1989 *Phys. Rev.* B **39** 2255
[34] Maeda F, Kawamura T, Oshima M, Hidaka Y and Yamaji A 1989 *Japan. J. Appl. Phys.* **28** L361
[35] Minami F, Kimura T and Takekawa S 1989 *Phys. Rev.* B **39** 4788
[36] Olson C G, Yang A B, Liu R, Gu C, Veal B W, Liu Z J, Paulikas A P, Vandervoort K, Arko A J and List R S 1989 *Int. Meeting on High Temperature Superconductivity (Stanford) July 1989* (Abstract 5B-79)
[37] Golden M S, Geeson D, Male S E and Flavell W R 1989 *Supercond. Sci. Technol.* **2** 185
[38] Geeson D A, Golden M S, Golden S J and Flavell W R 1989 *Supercond. Sci. and Technol.* **2** 279
[39] Sakisaka Y, Komeda T, Maruyama T, Onchi M, Kato H, Ajura Y, Yanahima H, Terashima T, Bando Y, Iijima K, Yamamoto K and Hirata K 1989 *Phys. Rev.* B **39** 2304
[40] Sakisaka Y, Komeda T, Maruyama T, Onchi M, Kato H, Ajura Y, Yanahima H, Terashima T, Bando Y, Iijima K, Yamamoto K and Hirata K 1989 *Phys. Rev.* B **39** 9080
[41] Roshko A and Chiang Y M 1989 *Preprint*
[42] Egdell R G, Harrison M R, Hill M D, Porte L and Wall G 1984 *J. Phys. C: Solid State Phys.* **17** 2889
[43] Kemp J P, Beal D J and Cox P A 1989 *J. Solid State Chem.* submitted for publication
[44] Egdell R G and Naylor P D 1982 *Chem. Phys. Lett.* **91** 200
[45] Owen I R, Brookes N B, Richardson C H, Warburton D R, Quinn F M, Norman D and Thornton G 1986 *Surf. Sci.* **178** 897
[46] Flavell W R and Egdell R G 1989 *Phys. Rev.* B **39** 231
[47] Dauth M B, Kachel T, Kupp B and Gudat W 1988 *Physica* C **153–155** 153
[48] Gourieux T, Krill G, Maurer M, Ravet M F, Menny A, Tolentino H and Fontaine A 1988 *Phys. Rev.* B **37** 7516
[49] Steiner P *et al* 1988 *Z. Phys.* B **69** 449
[50] Mori N, Takamo Y and Ozaki M 1987 *Japan. J. Appl. Phys.* **26** (suppl. 26-3) 1017
[51] Fink J, Nucker N, Romberg H and Fuggle J C 1989 *IBM J. Res. Dev.* in the press
[52] Ospelt M, Henz J, Kaldis E and Wachter P 1988 *Physica* C **153–155** 159
[53] Weaver J H, Meyer III H M, Wagener T J, Hill D M, Gao Y, Peterson D, Fisk Z and Arko A J 1988 *Phys. Rev.* B **38** 4668
[54] Ghijsen J, Tjeng L H, van Elp J, Eskes H and Czyzyk M T 1988 *Phys. Rev.* B **38** 11322
[55] Dai Y, Manthiram A, Campion A and Goodenough J B 1988 *Phys. Rev.* B **38** 5091
[56] Egdell R G and Hill M D 1983 *J. Phys. C: Solid State Phys.* **16** 6205
[57] Cox P A, Egdell R G, Goodenough J B, Hamnett and Naish C C 1983 *J. Phys. C: Solid State Phys.* **16** 6221
[58] Pickett W E 1989 *Rev. Mod. Phys.* **61** 433
[59] Takahashi T *et al* 1987 *Phys. Rev.* B **36** 5686
[60] Hufner S, Hulliger F, Osterwalder J and Riesterer T 1984 *Solid State Commun.* **50** 83
[61] Sawatzky G A and Allen J W 1984 *Phys. Rev. Lett.* **53** 2339
[62] Thuler M R, Benbow R L and Hurych Z 1982 *Phys. Rev.* B **26** 669
[63] Zhi-xun Shen *et al* 1987 *Phys. Rev.* B **36** 8414
[64] Takahashi T *et al* 1987 *Physica* C **148B** 476
[65] Kurtz R L, Stockbauer R L, Mueller D, Shih A, Toth L E, Osofsky M and Wolf S A 1987 *Phys. Rev.* B **35** 8818
[66] Onellion M, Chang Y, Niles D W, Joynt R, Margaitondo G, Stoffel N G and Tarascon J M 1987 *Phys. Rev.* B **36** 819
[67] Lowe A J *et al* 1988 *J. Phys. C: Solid State Phys.* **21** L763
[68] Samsavar A, Miller T, Chiang T-C, Pazol B G, Friedmann T A and Ginsberg D M 1988 *Phys. Rev.* B **37** 5164
[69] Shen Z-X, Lindberg P A P, Lindau I, Spicer W E, Eom C B and Geballe T H 1988 *Phys. Rev.* B **38** 7152
[70] Shen Z-X, Lindberg P A P, Soukiassian P, Eom C B, Lindau I, Spicer W E and Geballe T H 1989 *Phys. Rev.* B **39** 823
[71] Wendin G 1987 *J. Physique Coll.* **48** C9 1157
[72] Ramaker D E 1988 *Phys. Rev.* B **38** 11816
[73] Kurtz R L, Robey S W, Stockbauer R L, Mueller D, Shih A and Toth L 1989 *Phys. Rev.* B **39** 4768
[74] Qiu S L, Ruckman M W, Brookes N B, Johnson P D, Chen J, Lin C L, Strongin M, Sinkovic B, Crow J E and Cham-Soo Jee 1988 *Phys. Rev.* B **37** 3747
[75] Kurtz R L, Stockbauer R, Madey T E, Mueller D, Shih A and Toth L 1988 *Phys. Rev.* B **37** 7936
[76] Stoffel N G, Tarascon J M, Chang Y, Onellion M, Niles D W and Margaritondo G 1987 *Phys. Rev.* B **36** 3986
[77] Egdell R G 1985 *Adsorption and Catalysis on Oxide Surfaces* ed M Che and G C Bond (Amsterdam: Elsevier)
[78] Sarma D D, Prabhakaran K and Rao C N R 1988 *Solid State Commun.* **67** 263
[79] Jacobi K, Sarma D D, Geng P, Simmons C T and Kaindl G 1988 *Phys. Rev.* B **38** 863

[80] Fukuda Y, Nagoshi M, Suzuki T, Namba Y, Syono Y and Tachiki M 1989 *Phys. Rev.* B **39** 2760
[81] Reihl B, Riesterer T, Bednorz J G and Müller K A 1987 *Phys. Rev.* B **35** 8804
[82] Johnson P D *et al* 1987 *Phys. Rev.* B **35** 8811
[83] Thiry P, Rossi G, Petroff Y, Revcolevski A and Jegovdez J 1988 *Europhys. Lett.* **5** 55
[84] Egdell R G and Flavell W R 1989 *Z. Phys.* B **74** 279
[85] Steiner P, Hufner S, Jungmann A, Junk S, Kinsinger V, Sander I, Theile W R, Backes N and Politis C 1988 *Physica* C **156** 213
[86] Michel E G, Alvarez J, Asensio M C, Miranda R, Ibanez J, Peral G, Vicent J L, Garcia F, Moran E and Alario-Franco M A 1988 *Phys. Rev.* B **38** 5146
[87] Hill D M, Meyer H M III, Weaver J H, Gallo C F and Goretta K C 1988 *Phys. Rev.* B **38** 11331
[88] Doniach S and Sunjic M 1970 *J. Phys. C: Solid State Phys.* **3** 285
[89] Tanaka M, Takahashi T, Katayama-Yoshida H, Yamazaki S, Fujinami M, Okabe Y, Mizutani W, Ono M and Kijimura K 1989 *Nature* **339** 691
[90] Cranstoun G K L, Egdell R G, Hill M D and Samson R 1984 *J. Electron Spectrosc. Relat. Phenom.* **33** 23
[91] Chang Y *et al* 1989 *Phys. Rev. Lett.* submitted for publication
[92] Gallagher M C, Adler J G, Jung J and Franck J P 1988 *Phys. Rev.* B **37** 7846
[93] Bonn D A, O'Reilly A H, Greedan J E, Stager C V, Timusk T, Kamaras K and Tanner D B 1988 *Phys. Rev.* B **37** 1574